20

Collective Motion of Multi-Robot System based on Simple Dynamics

Ken Sugawara[1], Yoshinori Hayakawa[2], Tsuyoshi Mizuguchi[3] and Masaki Sano[4]
[1]*Tohoku Gakuin University,* [2]*Tohoku University,* [3]*Osaka Prefecture University,* [4]*University of Tokyo*
Japan

1. Introduction

Multi-robot system is one of the most attractive systems in robotics, and many researchers have been investigating it from various viewpoints (Cao, 1997; Balch & Parker, 2002; Parker, 2003). Remarkable point of multi-robot system is that the robots are cooperatively able to complete a task that a single robot can hardly or cannot accomplish by itself. Especially, searching, transportation or conveyance, construction, and pattern formation are typical categories which are suitable for multi-robot system, and a lot of concrete tasks can be found in each category. Some approaches have been considered and proposed to accomplish them, and biology inspired robotics is one of the most effective method to develop useful multi-robot system. Actually, many researchers have been applying this approach to design multi-robot system (Bonabeau, 1999).

In this article, we treat collective motion of motile elements which was inspired by living things such as fishes, birds and small insects, assuming to apply to real robot system. It is considered that the collective motion of the robots can be utilized for some significant tasks such as traffic control, ground/ocean surveillance (Ogen, 2004), and so on.

This article is organized as follows. In section 2, we explain a fundamental kinetic model of collective behaviors based on the livings. Result of numerical simulation and analysis are shown in Section 3. In section 4, we show small scale of experiment based on the model.

2. Kinetic model for collective motions

Many animals form groups which we consider as cooperative systems of active elements. The collective motions of animals show extreme diversity of dynamics and patterns (Edelstein-Keshet, 1990; Partridge, 1982; Wilson 1975) For example, migrant fish, like the sardine, tend to school by aligning their headings and keeping a fixed mutual distance. Large birds such as cranes migrate in well-ordered formations with constant cluster velocity. Small birds such as sparrows fly in wandering, disordered aggregates. Insects, such as the mosquito, fly at random within spatially limited swarms. There seems a tendency that the smaller the size of animals, the more disorder in cluster motions, at least, for some flying or swimming animals. Many model equations claim to explain the collective motions of

Source: Human-Robot Interaction, Book edited by Nilanjan Sarkar,
ISBN 978-3-902613-13-4, pp.522, September 2007, Itech Education and Publishing, Vienna, Austria

animals (Niwa, 1994; Doustari & Sannomiya, 1992; Vicsek *et al.*, 1995). Most postulate that individuals are simply particles with the mutual interactions and motive force. In this simplification, the equations of motion become Newtonian equations for the particles, and the dependence on the characteristic scales of animals appears only through their mass. The resulting collective motions are mostly regular and ordered. Swarming, disordered aggregates and wandering, require external random perturbations.

To generalize these models, we introduce extended internal variables describing the particles, which we call motile elements (Shimoyama *et al.*, 1996). Basically, the motion of *i*-th element is described with a position vector $\vec{r}_i$ and a velocity vector $\vec{v}_i$ which are relative to fluid or air. Although the internal variables may have physical, physiological or ecological origins in each species, we additionally use a simple physical vector degree of freedom; the *heading unit vector* $\vec{n}_i$, parallel to the axis of the animal. Large birds often glide. In a glide, the heading, $\vec{n}_i$, and the velocity vector, $\vec{v}_i$, need not be parallel. Therefore, we assume that $\vec{n}_i$ and $\vec{v}_i$ relax to parallel with relaxation time τ. Including the heading dynamics, we propose a kinetic model of N interacting motile elements. For simplicity, we consider two-dimensions, but the model is easily extensible to three-dimensions. The state variables for the *i*-th element are the position vector $\vec{r}_i$, the velocity vector $\vec{v}_i$, and the heading unit vector $\vec{n}_i$, and these variables have the following dynamics:

$$m\frac{d\vec{v}_i}{dt} = -\gamma\vec{v}_i + a\vec{n}_i + \sum_{j\neq i}\alpha_{ij}\vec{f}_{ij} + \vec{g}_i \tag{1}$$

$$\tau\frac{d\theta_i}{dt} = \sin(\phi_i - \theta_i) + \sum_{j\neq i} J_{ij}\sin(\theta_j - \theta_i) \tag{2}$$

$$(i = 1,2,\cdots,N)$$

where θ_i is the angle between the unit vector $\vec{n}_i$ and a certain direction, say, the x axis ($\vec{n}_i = (\cos\theta_i, \sin\theta_i)$), and ϕ_i is the angle between the velocity vector $\vec{v}_i$ and the x axis($\vec{v}_i = |\vec{v}_i|(\cos\phi_i, \sin\phi_i)$) (Fig.1).

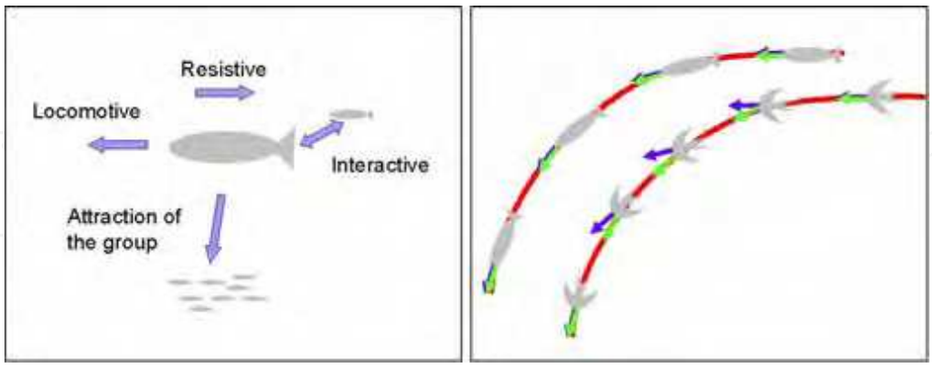

Figure 1. Schematic diagram for Newton's equation of motion for particles (left) , and the dynamics of the heading (right). The relaxation time τ of birds is much larger than that of fishes

In this model, every element is identical except for initial conditions. Eq.(1) is Newton's equation of motion for particles of mass *m*, is the resistive coefficient based on Stokes's law for an element moving in fluid. We assume that the motile force *a* acts in the heading direction $\vec{n}_i$. The term $\vec{f}_{ij}$ represents mutual attractive and repulsive forces between the *i*-th and *j*-th elements, and $\vec{g}_i$ is the force toward the center of group, which is taken as the gravitational center in our model. We use the analogy with the intermolecular forces as introduced by Breder (1954) based on the observations for fish schooling (see also (Aoki, 1980; Breder, 1976)). We assume that the interaction force is given by:

$$\vec{f}_{ij} = -c\left\{\left(\frac{\left|\vec{r}_j - \vec{r}_i\right|}{r_c}\right)^{-3} - \left(\frac{\left|\vec{r}_j - \vec{r}_i\right|}{r_c}\right)^{-2}\right\}\cdot\left(\frac{\vec{r}_j - \vec{r}_i}{r_c}\right)\cdot \exp(-\left|\vec{r}_j - \vec{r}_i\right|/r_c), \tag{3}$$

where *c* is a parameter that represents the magnitude of interactions and r_c the optimal distance between neighbors.
The interaction need not be isotropic. If the interaction is based on visual information, the interaction with elements in front of a given element is stronger than with those behind. Therefore, we introduce a direction sensitivity factor described by:

$$\alpha_{ij} = 1 + d\frac{\vec{n}_i \cdot (\vec{r}_j - \vec{r}_i)}{\left|\vec{r}_j - \vec{r}_i\right|}$$

$$(0 \le d \le 1) \tag{4}$$

or

$$\alpha_{ij} = 1 + d\cos\Phi, \tag{4'}$$

where Φ implies the angle formed by $\vec{n}$ and $\vec{r}_j - \vec{r}_i$. Here a new parameter *d* is introduced to control the anisotropy of sensitivity. When *d*=0, the interaction is isotropic.

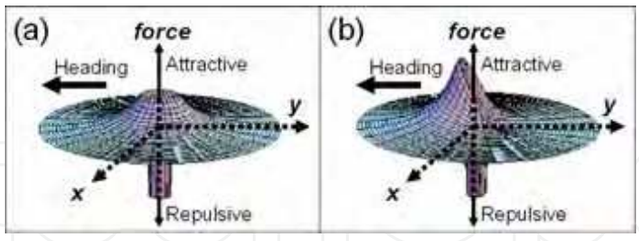

Figure 2. Schematic images of interaction force. (a) in case of *d*=0. (b) in case of *d*=1

Furthermore, we introduce a global attraction force $\vec{g}_i$ given by:

$$\vec{g}_i = c_g\frac{\vec{g} - \vec{r}_i}{N\left|\vec{g} - \vec{r}_i\right|} \tag{5}$$

where $\vec{g}_i$ is the center of group, *i.e.*,

$$\vec{g} = \sum_i \vec{r}_i / N \tag{6}$$

In the following discussions, we assume these two interaction forces have the same order of magnitude, *i.e.*, $c = c_g$.

The velocity vector $\vec{v}_i$ need not be in the heading direction $\vec{n}_i$, because of the inertial moment of the animal's body. We assume that the heading is parallel to the velocity for linear motion. We use equation (2) to relax the difference between the heading angle and the velocity direction angle. The relaxation time τ is related to the inertial moment and drag of the animal's body, and the time scale of maneuvering, such as the flapping period of wings or fins for birds or fishes, or tumbling period of flagella for bacteria. If the individuals are small (the inertial moment is small) and fast in flapping, τ is small (Fig.1 (right)).

To account for the tendency of animals to align their heads (Inoue, 1981; Hunter, 1966), we consider the interaction of $\vec{n}_i$ vectors. In the second term of the right hand side of Eq. (2), J_{ij} represents the tendency of individual i to align with individual j. We assume here that the interaction is a decreasing function of distance,

$$J_{ij} = k\left(\frac{|\vec{r}_j - \vec{r}_i|}{r_c}\right)^{-1} \tag{7}$$

However, in the most of the present work we take $k=0$ if not specified.

3. Numerical simulations and experiments

3.1 Characteristic of collective behavior

To investigate the qualitative properties of our model, we carried out numerical simulations for various control parameters and observed the collective motions. The equations of motion were solved with an explicit Euler method. Typical value of Δt to avoid numerical instability was less than 0.01. Initially, motile elements are placed at random by using Gaussian distributed random vectors in two dimensions within the standard deviation on the order of the inter-neighbour distance, r_c. The initial velocity of the elements is also given by Gaussian distributed random vectors with standard deviation of unity, and the heading vectors $\vec{n}$ are set in random directions.

We carried out numerical simulation for N ranging from 10 to 100, and we found several distinct collective behaviors which can be seen independently to $N < 100$. The trajectory of the center of the cluster are illustrated in Fig. 3. The trajectories are classified into four types.

1. **Marching:** When the anisotropy of mutual attraction is small, the elements form a regular triangular crystal moving at constant velocity. The formation is stable against disturbance and velocity fluctuations are very small. We call this motion a marching state.
2. **Oscillation:** Several group motions exhibit regular oscillations, including:
   (i) Wavy motion of the cluster along a linear trajectory.
   (ii) A cluster circling a center outside the cluster.
   (iii) A cluster circling a center inside the cluster.

The stability of oscillatory motion is weaker than that of marching. Oscillatory clusters often occur near the boundary between wandering, and the oscillation and marching may coexist for some parameters.

3. **Wandering:** For non-zero d, the center of the cluster can wander quite irregularly, while the lattice-like order inside the cluster persists. The mutual position of elements rearranges intermittently according to chaotic changes in the direction of motion. We call this behavior wandering. It occurs in flocks of birds, e.g., small non-migratory birds like the sparrow.
4. **Swarming:** Beyond the wandering regime, we found more irregular motion, where the regularity within the cluster fails, although the cluster persists. Compared to wandering, the velocity of elements has a wide distribution, and the mobility of the cluster is small, a behavior reminiscent of a cloud of mosquitoes.

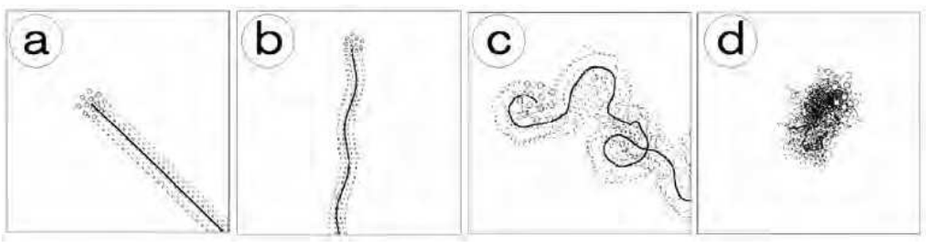

Figure 3. The trajectories of the elements (dotted lines) and the center of mass (solid line) obtained by numerical simulation. Each cluster consists of twelve motile elements (shown as white circle). Typical types of collective motions are shown as: (a) marching, (b) oscillatory (wavy), (c) wandering, and (d) swarming

Marching and oscillation form an ordered phase, while the others form a disordered phase. In the ordered phase, elements behave as a regularly moving cluster which is stable against perturbations by external force or small changes of kinetic parameters. This kind of stability would be required for the grouping animals, too, because the cluster of traveling birds or fishes should be structural stable. On the contrary, in disordered phase, the motion of clusters become unpredictable, which would be beneficial for small animals to escape from predators.

We refer to the transition between order and disorder as the marching/swarming transition. We have examined the parameter dependence of the behavior, fixing the number of elements, $N = 10$. In Fig. 4, we show characteristic behaviors in τ - γ and τ - a space. Fig. 4(a) shows that the transition between marching and wandering is well defined and the boundary occurs when $\gamma/\tau \sim 20$. Since γ is proportional to the relaxiation time in velocity, γ/τ gives the ratio of characteristic time for heading reoriantation and velocity relaxiation of individual elements. Fig. 4(b) shows that the transition line is approximately $a \sim \tau^{-1/2}$, which seems to be nontrivial.

From similar plots, We obtain $r_c \sim \tau$ and $c \sim \tau$ as transition lines. The former can be interpreted as the balancing of collision time between neighboring elements and heading relaxiation time, and the later the balancing of velocity and heading relaxations. These proportionalities suggest that we use dimensionless parameters. Futhermore, we expect that the proportionalities would held for larger N>10, while the factors, *i.e.*, the positions of

transitions, might change. However, more specific transition lines, such as wandering/ swarming, are difficult to draw without introducing proper order parameters.

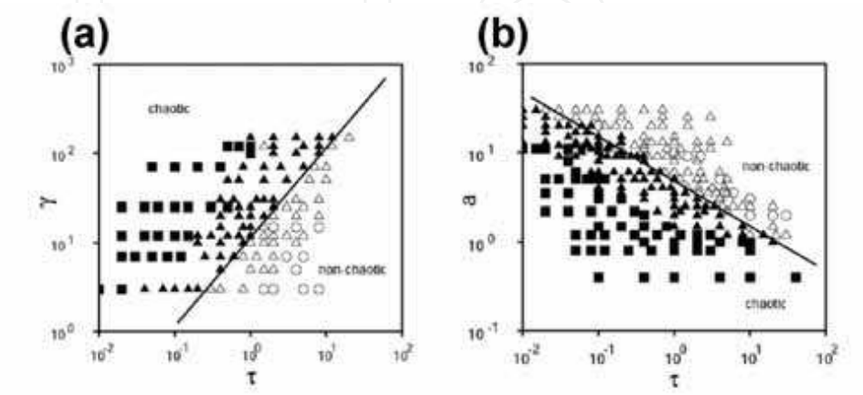

Figure 4. Parameter dependence of collective behavior. (a) γ versus τ. (b) *a* versus τ. Here, white circles indicate marching, white triangles oscillation, black triangles wandering, and black rectangles swarming

3.2 Dimensionless parameters

Next, we derive the dimensionless representation of our model and classify its behaviors. To reduce the model equation to a dimensionless form, we rescale each variable by a characteristic dimension: the characteristic length $L_0 \equiv r_c$ is comparable to the size of each individual, the steady state velocity $V_0 \equiv a/\gamma$ of elements, and the characteristic time $T_0 \equiv L_0 / V_0 = r_c \gamma / a$. Introducing the non-dimensional variables v', t', r' defined by $v = V_0 v'$, $t = T_0 t'$, $r = L_0 r'$, we obtain the following non-dimensional equations of motion for the *i*-th element (Shimoyama *et al.*, 1996):

$$\frac{d\vec{v}_i'}{dt'} = \frac{1}{R}(-\vec{v}_i' + \vec{n}_i - \frac{1}{Q}\sum_{j \neq i} \alpha_{ij} \vec{f}_{ij}), \tag{8}$$

$$\frac{1}{P}\frac{d\theta_i}{dt'} = \sin(\phi_i - \theta_i) + \sum_{j \neq i} J_{ij} \sin(\theta_j - \theta_i). \tag{9}$$

We have three independent dimensionless parameters *P*,*Q* and *R* defined by:

$$P \equiv \frac{r_c \gamma}{a\tau}, \quad Q \equiv \frac{a}{c}, \quad R \equiv \frac{ma}{\gamma^2 r_c}. \tag{10}$$

The physical interpretation of each parameter is: *P* is the ratio of the typical time scale for heading relaxation, τ and the "mean free time", $r_c\gamma/a$. *Q* is the ratio of the magnitude of the motive force and the interaction force with neighbors. *R* is the ratio of the inertial force and the viscous force, which is resembles a "Reynolds number" in fluid mechanics.

3.3 Phase diagram

We now review the numerical results, focusing on the marching/swarming transition, in the viscous regime where R < 0.05. Consider the dependence of the marching/swarming transition line in the phase diagram given in the previous section. At the transition line, we obtained $\gamma^* \sim \tau^*$, $a^* \sim \tau^{*-1/2}$, $c^* \sim \tau^*$, and $r_c^* \sim \tau^*$, where * signifies the boundary between the states. Using a new dimensionless parameter defined by $G \equiv P/Q$, these relations simplify to

$$G = \frac{r_c^* \gamma^* c^*}{a^{*2} \tau^*} = const. \tag{11}$$

as shown in Fig. 5. All data from independent numerical simulations collapse onto the same representation, with the transition line at $G^*=const$.

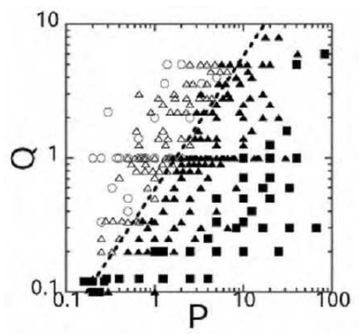

Figure 5. Phase diagram of collective motions in the viscous regime (R < 0.05) obtained by independent numerical simulations by changing parameters (*P versus Q*). In the diagram, white circles indicate marching, white triangles oscillation, black triangles wandering, and black rectangles swarming

3.4 Degree of disorder

To characterize the different collective motions quantitatively, we need suitable measures of disorder, *i.e.*, disorder parameters. In ordered motions (marching and oscillating), the trajectory of each element occupies a very limited region in velocity space. In chaotic motions, both temporal fluctuations of cluster velocity and velocity deviations of elements are large. Thus, we can define several disorder parameters. Letting the velocity of the cluster at a moment t be,

$$\vec{V}(t) = \frac{1}{N} \sum_i \vec{v}_i(t), \tag{12}$$

the fluctuation in velocity space can be evaluated by averaging the root mean square (*r.m.s.*) velocity deviation over time;

$$\left\langle (\Delta v)^2 \right\rangle \equiv \left\langle \frac{1}{N} \sum_i \left| \vec{v}_i(t) - \vec{V}(t) \right|^2 \right\rangle_t . \tag{13}$$

We can define a similar parameter, the fluctuation of $V(t)$ over time, by

$$\left\langle (\Delta V)^2 \right\rangle \equiv \left\langle \left(\vec{V}(t) - \left\langle \vec{V}(t) \right\rangle_t \right)^2 \right\rangle_t . \tag{14}$$

Both quantities are zero in ordered motions and non-zero in disordered motions. In the vicinity of the marching/swarming transition we calculated these quantities as a function of G as shown in Fig. 6. In the plot, both quantities are normalized by the average cluster velocity $<V^2>$, and the square root of the values is shown. Using these parameters, the order-disorder transition appears as a change in the disorder parameters. $<(\Delta V)^2>^{1/2}$ and $<(\Delta v)^2>^{1/2}$ are a feasible way to characterize ordered vs. disordered motions. Above the transition, the transition point, G^*, $<(\Delta v)^2>^{1/2}/<(\Delta V)^2>^{1/2}$ increases because the fluctuation of cluster motion approaches the cluster velocity. Fluctuations inside the cluster increase continuously as G increases. Swarming state corresponds to $<(\Delta V)^2>^{1/2}/<V^2>^{1/2} > 1$ and wandering and swarming states are continuous. It should be noted that the transition becomes sharper as N increases. The transition point G^* does not change. This suggests that the same transition can be seen for larger size of groupings.

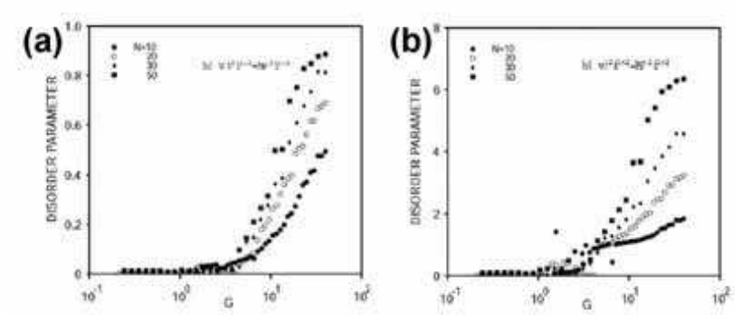

Figure 6. Characterization of the marching wandering transition in the viscous regime using disorder parameters. (a) $<(\Delta V)^2>^{1/2}/<V^2>^{1/2}$ and (b) $<(\Delta v)^2>^{1/2}/<(\Delta V)^2>^{1/2}$. The plots are made for several clusters of different size N from 10 to 50

3.5 Modification for formation control

Proposed model described above shows a variety of the group motions, however, it only shows a regular triangular crystal formation and its boundary is round when we focus on the formation of the group. In nature, we can observe other type of formations as well as spherical structure observed in small fish school or the swarms of small insects. Large migratory birds tend to form linear structure, which is considered to be hydrodynamically advantageous. In robotics, there are some researches which focus on the formation control of multi-robot (Balch & Arkin, 1998; Fredslund, 2002; Jadbabaie, 2003; Savkin, 2004), and most of them introduce a kind of geometrical formation rules.

Our interest is to express not only round-shaped structure but also other formations by modifying the above-mentioned model. In this section, modified model for formation control is explained, especially focusing on form of linear structure. Note that we just treat Newton's equation of motion for particles and do not treat geometrical rules.

The direction sensitivity is controlled by the parameter d in Eq.(4). From the simple analysis, we know that it is better to strengthen the direction sensitivity for linear formation. One of

the simplest way to strengthen the direction sensitivity is to use d^2 instead of d in Eq.(4). But for more drastic modification, we found it is more effective to replace r_c with $\alpha_{ij} \cdot r_c$ instead of strengthen d. Schematic images of interaction force are shown in Fig.7.

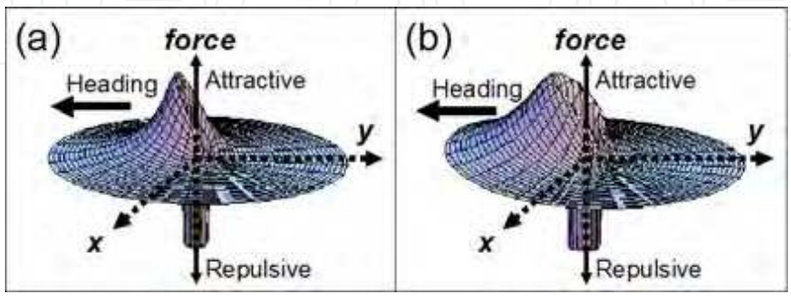

Figure 7. Images of interaction force in case of d=1, (a) r_c=*const.*, (b) r_c=a_{ij} x *const*

Fig.8 shows a typical behavior of the system based on the modified model. As you see, they organize a double line structure. This formation is stable and robust to perturbation.

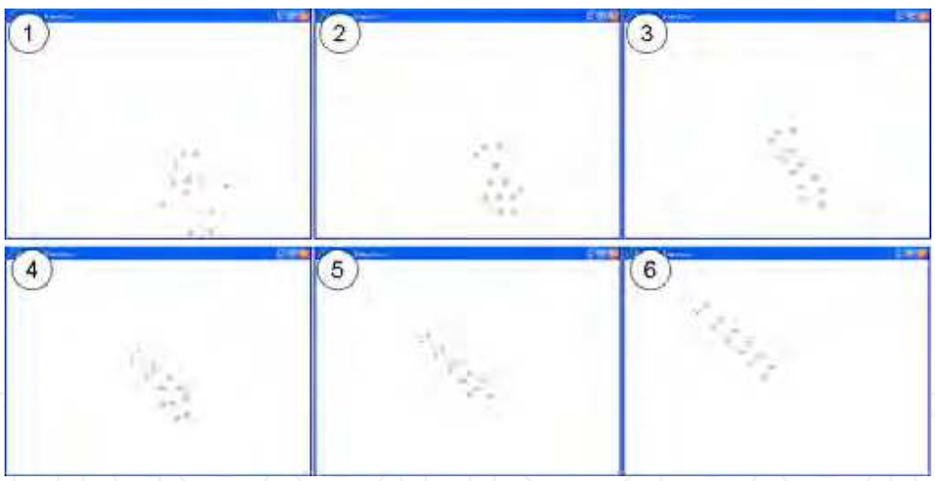

Figure 8. Self-organization of double line structure

We can also show that the angle between the forward direction and double line structure can be controled independently by modifying direction sensitivity.

$$\alpha_{ij} = 1 + d\cos(\Phi + \delta). \tag{15}$$

we can design the heading angle by δ. Fig.9 shows the process that the double line structure is organized, in which heading angle is controlled as $\delta = \pi/6$.

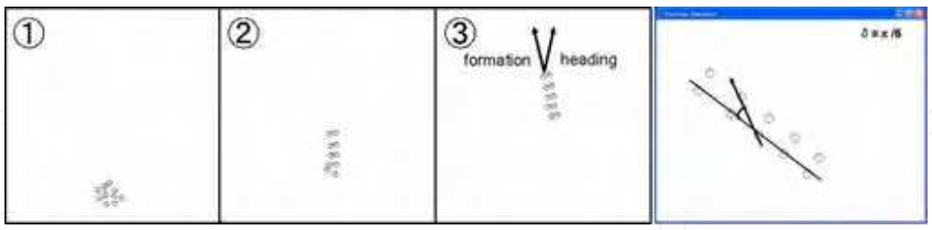

Figure 9. Self-organization of double line structure in case of $\delta=\pi/6$

4. Robot experiment

4.1 Collective behavior of the group

Performance of this system is also confirmed by the experiment of real robot system. Miniature mobile robots Khepera, which is one of the most popular robots for experiments, are used here. As the sensors on the robot are insufficient to measure the direction and the distance between the robots, positions and directions of the robot are measured by the overhead camera and each robot determines its behavior based on this information.

The model contains a degree of freedom for the heading. Khepera robot, however, has no freedom for heading. So we divide the movement of the robots into two phases: the phase to update the position, and the phase to update their directions. Fig. 10 shows the snapshot of the experiment and the trajectories of the robots in case of "marching", "Oscillatory", and "wandering."

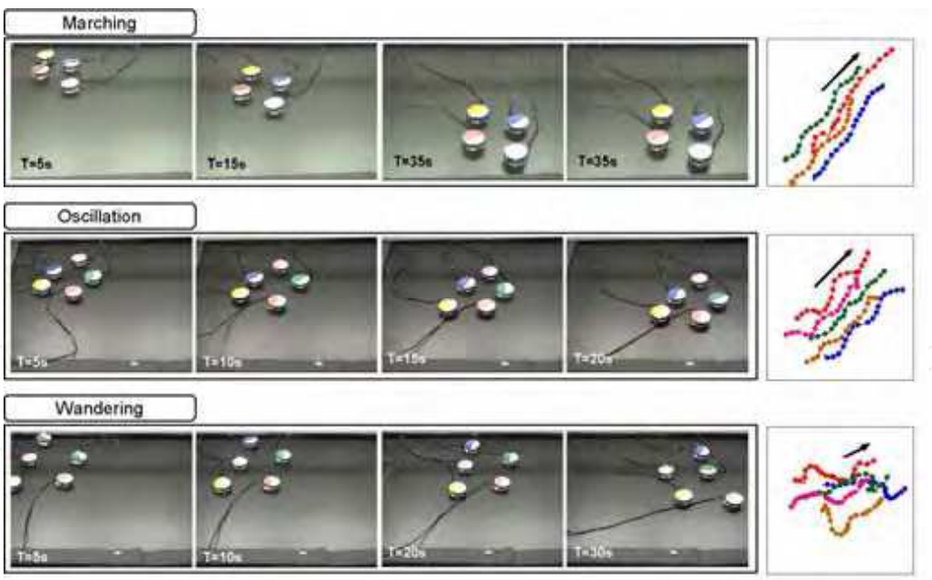

Figure 10. Snapshots of the experiment in case of "marching", "oscillatory" and "wandering" behaviour (pictures), and trajectories of the robots (plots)

4.2 Double line formation

The performance of the modified model is also confirmed by the robot experiment. The condition of the experiment is same as previous section. Fig.11 shows the snapshot of the experiment and the trajectories of the robots. We can see the robots organize double line formation.

Figure 11. Snapshots of the experiment in case of "double line formation"

5. Summary

In this article, we proposed a mathematical model which show several types of collective motions, and validated it. Firstly we constructed a model in which each element obeys the Newton equation with resistive and interactive force and has a degree of freedom of the heading vector which is parallel to the element axis, in addition to its position and velocity. Performance of the model was confirmed by numerical simulation, and we obtained several types of collective behavior, such as regular cluster motions, chaotic wandering and swarming of cluster without introducing random fluctuations. By introducing a set of dimensionless parameters, we formulated the collective motions and obtained the phase diagram and a new dimensionless parameter G. Lastly, we referred to the behaviour of extended model in which the anisotropy of the interaction force is modified, and showed the group organizes the double line formation.

6. References

Aoki, I. (1980). An Analysis of The Schooling Behavior of Fish: Internal Organization and Communication Process, *Bull. Res. Inst. Univ. Tokyo*, 12, pp.1-65.

Balch, T. & Arkin, R. C. (1998). Behavior-Based Formation Control for Multiagent Robot Teams, *IEEE Trans. on Robotics and Automation*, Vol.14, No.6, pp.926-939.

Balch, T. & Parker, L. E. (2002). *Robot Teams : From Diversity to Polymorphism*, A K Peters Ltd, ISBN:9781568811550

Bonabeau, E., Dorigo, M., & Theraulaz, G. (1999), *Swarm Intelligence: From Natural to Artificial Systems*, Oxford University Press, New York, ISBN:0-19-513159-2

Breder, C. M. (1954). Equations Descriptive of Fish Schools and Other Animal Aggregations, *Ecology*, 35, pp.361-370

Breder, C. M. (1976). Fish Schools as Operational Structures, *Fish. Bull.*, 74, pp.471-502.

Cao, Y. U., Fukunaga, A. S. and Kahng, A. B. (1997), "Cooperative Mobile Robotics: Antecedents and Directions, *Autonomous Robots*, 4, pp.7-27.

Doustari, M. A. & Sannomiya, N. (1992). A Simulation Study on Schooling Mechanism in Fish Behavior, *Trans. ISCIE*, 5, pp.521-523.

Edelstein-Keshet, L. (1990). Collective motion, In: *Lecture Notes in Biomathematics*, Alt, W. & Hoffmann, G., (Ed), pp.528-532.

Fredslund, J. & Mataric, M. J. (2002). A General, Local Algorithm for Robot Formations, *IEEE Trans. on Robotics and Automation*, Vol.18, No.5, pp.837-846.

Hunter, J. R.(1966). Procedure for Analysis of Schooling Behavior. *J. Fish. Res. Board Canada*, 23, pp.547-562.

Inoue, M. (1981). *Fish school; behavior* (in Japanese). Tokyo:Kaiyo-shuppan.

Jadbabaie, A., Lin, J. & Morse, A. S. (2003). Coordination of Groups of Mobile Autonomous Agents Using Nearest Neighbor Rules, *IEEE Trans. on Automatic Control*, Vol.48, No.6, pp.988-1001.

Niwa, H. (1994). Self-organizing Dynamic Model of Fish Schooling. *J. of Theor. Biol.*, 171, pp.123-136.

Ogren, P., Fiorelli, E. & Leonard, N. E. (2004). Cooperative Control of Mobile Sensor Networks: Adaptive Gradient Climbing in a Distributed Environment, *IEEE Transactions on Automatic Control*, Vol.49, No.8, 2004, pp.1292-1302.

Parker, L. E. (2003). Current Research in Multirobot Systems, *Artificial Life and Robotics*, vol. 7, pp.1-5.

Partridge, B. L. (1982). The Structure and Function of Fish Scholls. *Sci. Am.* 246, pp.90-99.

Savkin, A. (2004) Coordinated collective motion of groups of autonomous mobile robots: Analysis of vicsek's model, *IEEE Trans. on Automatic Control*, Vol.49, No.6, pp.981-983.

Shimoyama N., Sugawara K., Mizuguchi T., Hayakawa Y., Sano M. (1996). Collective Motion of a System of Motile Elements, *Phys. Rev. Lett.*, 79, pp.3870-3873.

Vicsek, T., Czirok, A., Ben-Jacob, E., Cohen I., & Shochet, O. (1995). Novel Type of Phase Transition in a System of Self-Driven Particles. *Phys. Rev. Lett.*, 75, pp.1226-1229.

Wilson, E. O. (1975). *Sociobiology*, Harvard.

Human Robot Interaction

Edited by Nilanjan Sarkar

ISBN 978-3-902613-13-4

Hard cover, 522 pages

Publisher I-Tech Education and Publishing

Published online 01, September, 2007

Published in print edition September, 2007

Human-robot interaction research is diverse and covers a wide range of topics. All aspects of human factors and robotics are within the purview of HRI research so far as they provide insight into how to improve our understanding in developing effective tools, protocols, and systems to enhance HRI. For example, a significant research effort is being devoted to designing human-robot interface that makes it easier for the people to interact with robots. HRI is an extremely active research field where new and important work is being published at a fast pace. It is neither possible nor is it our intention to cover every important work in this important research field in one volume. However, we believe that HRI as a research field has matured enough to merit a compilation of the outstanding work in the field in the form of a book. This book, which presents outstanding work from the leading HRI researchers covering a wide spectrum of topics, is an effort to capture and present some of the important contributions in HRI in one volume. We hope that this book will benefit both experts and novice and provide a thorough understanding of the exciting field of HRI.

InTech Europe

University Campus STeP Ri
Slavka Krautzeka 83/A
51000 Rijeka, Croatia
Phone: +385 (51) 770 447
Fax: +385 (51) 686 166
www.intechopen.com

InTech China

Unit 405, Office Block, Hotel Equatorial Shanghai
No.65, Yan An Road (West), Shanghai, 200040, China
中国上海市延安西路65号上海国际贵都大饭店办公楼405单元
Phone: +86-21-62489820
Fax: +86-21-62489821

IntechOpen